

Disordered insulator in an optical lattice

M. Pasienski¹, D. McKay¹, M. White¹, and B. DeMarco¹

¹ *Physics Department, University of Illinois, 1110 W Green St, Urbana, IL 61801*

Disorder can profoundly affect the transport properties of a wide range of quantum materials. For example, the superfluid transition temperature for helium is strongly modified when it is adsorbed in porous media¹, disorder can generate insulating and metallic states in superconducting thin films², and understanding how disorder affects the emergence of high-temperature superconductivity is a problem with critical implications for both practical applications and fundamental condensed matter physics³. Presently, there is significant disagreement regarding the effect of disorder on transport in the disordered Bose-Hubbard (DBH) model—the paradigm used to theoretically study disorder in strongly correlated bosonic systems⁴. We experimentally realize the DBH model by using optical speckle to introduce precisely known, controllable, and fine-grained disorder to an optical lattice⁵. Here, we show that disorder can induce a SF-to-insulator (IN) transition in this system, but we find no evidence for a disorder-generated IN-to-SF transition, in conflict with certain theoretical predictions. We find that the transition to an IN is marked by changes in both the quasimomentum distribution and the dissipation strength for transport. We probe the quasimomentum distribution using time-of-flight (TOF) imaging⁶, and the transport properties by measuring the motion of the centre-of-mass (COM) of the atom gas immediately after an applied impulse⁷. By correlating these measurements, we determine that the transition from a SF to an IN is associated with the complete destruction of the condensate by disorder and the emergence of a localized state. We find that increasing disorder strength generically leads to greater dissipation in the regime of mixed SF and Mott-insulator (MI) phases,

ruling out theories that predict a disorder-induced MI-to-SF transition for this system.

A wide range of sophisticated theoretical approaches applied to determine the ground state phase diagram of the DBH model have reached inconsistent conclusions (see Refs. 4 and 8 for an overview and 9–12 for recent results). Precisely how insulating phases arise as microscopic parameters—such as the disorder strength, interaction energy, tunnelling energy, and chemical potential—are varied is presently a subject of intense debate, particularly for three-dimensional systems. Resolving these issues by comparison to measurements on solids is complicated by incomplete knowledge of the physical disorder and the influence of other degrees of freedom, such as lattice distortions and long-range electronic interactions. The schematic phase diagrams shown in Figs. 1a and b summarize the mutually conflicting results obtained by different computational and theoretical methods. A primary point of contention is whether applying disorder can transform the Mott-insulating (MI) phase only into a Bose-glass (BG) phase (Fig. 1a, e.g., Refs. 11,13,14) or also into a SF phase (Fig. 1b, e.g., Refs. 9,10,12,15). The BG phase—a compressible, gapless IN first discussed in Ref. 16—has yet to be unambiguously observed in an experiment.

Ultra-cold atom gases confined in disordered potentials have recently emerged as an ideal system for exploring these fundamental questions^{4,17}. Disorder can be controllably introduced using an optical speckle field^{18,19–21}; the disorder strength can be continuously varied by changing the optical intensity, and precise characterization of the disordering potential is possible using high-resolution microscopy. Because the interactions between atoms can also be manipulated, the effects of disorder can be explored both in the non-interacting regime and in the strongly correlated limit. For example, Anderson localization in a disordered potential generated by speckle²² and in a quasi-crystalline system²³ has been observed, and we have realized the DBH model in

the strongly interacting regime by combining optical speckle with a three-dimensional optical lattice⁵.

In our experiment, ⁸⁷Rb Bose-Einstein condensates are confined in a disordered optical lattice created by three pairs of 812 nm laser beams and a 532 nm optical speckle field, as described in Ref. 5. Figure 2a shows the relative geometry of the lattice beams (red lines) and disordering potential (green arrow) projected onto the plane used to image the atom gas. We control the ratio of interaction energy U to tunnelling energy t for the atoms by tuning the lattice potential depth, which is characterized by a dimensionless parameter s (the lattice potential depth is sE_R along each lattice direction, where E_R is the atomic recoil energy at 812 nm). The speckle potential is cylindrically symmetric with characteristic speckle sizes 570 nm and 3 μm along the transverse and longitudinal directions to propagation; sample slices through the measured speckle intensity profile are shown in green in Fig. 2a. Because the disorder in our experiment is fine grained (i.e., smaller than two 406 nm lattice spacings along any lattice direction), the speckle potential leads to a distribution of Hubbard site occupation, tunnelling, and interaction energies (see Ref. 5). We characterize the strength of the disorder Δ by the average potential shift from the speckle field, which is equivalent to the standard deviation of the site occupation energy distribution. In contrast to our previous work in the high filling limit⁵, we adjust the atom number so that approximately one particle occupies each site in the centre of the lattice for all of the data reported here.

The effect of disorder on condensate fraction and the atomic quasimomentum distribution is shown using representative images taken after bandmapping⁶ and TOF for $s=6$ and 12 in Fig. 2. The black and white bars indicate the diameters of the narrow condensate and broad non-condensate (NC) components, respectively. As we previously observed in the high filling limit, increasing Δ depletes the condensate into a

NC component consisting of atoms in high quasimomentum states. At $s=6$, well into the SF regime of the clean BH model, the NC populated by applying strong disorder ($\Delta = 3E_R$) reflects the symmetry of the speckle field, with a diameter approximately twice as large along the transverse direction (Fig 2b). Dramatic behaviour is evident in the quantum depleted SF regime at $s=12$: the condensate is completely destroyed by strong disorder (Fig. 2d), giving way to a spherically symmetric and broad quasimomentum distribution. This effect is unrelated to heating of the atom gas, since the condensate fraction recovered after slowly turning down the disordered lattice is not significantly affected for the range of Δ used in this work. The quasimomentum distribution in Fig. 2d closely resembles the distribution deep in the MI regime, in which the atoms have equal quantum amplitude at all quasimomentum, and hence the atomic wavefunctions are entirely localized (aside from small corrections related to finite tunnelling energy²⁴). The transport measurements shown in Fig. 3 verify the implication that the localized state observed in Fig. 1d is an IN.

One way to understand the effects of disorder observed in Figs. 2b,d is using a simple model (shown schematically in Fig. 2e) in which atoms localize to screen the disorder through interactions^{8,15,25}. A random distribution of site energies—indicated by black lines in Fig. 2e—would result in high kinetic energy states localized into the deepest lattice wells for non-interacting particles. The strong repulsive interactions present in this many-particle system, however, prevent multiple occupation of these localized states. Instead, only a fraction of the atoms localize into the deepest wells, leading to a corresponding reduction of condensate fraction. The remaining atoms exist in a delocalized, lower energy SF state because they experience a more uniform effective potential (red lines in Fig. 2e) arising from their interactions with the localized atoms. The asymmetry of the NC at $s=6$ is a direct result of the difference in speckle correlation length scales along the transverse and longitudinal directions: in contrast to the transverse direction for which energy shifts are uncorrelated from site-to-site, the

atoms can localize to a several-site-region to screen the disorder along the longitudinal direction. The quasimomentum distribution of the disorder-induced NC is therefore narrower along the longitudinal direction. At $s=12$, the atoms are mostly localized into single sites in the clean lattice through quantum depletion, so that additional disorder-induced localization can lead to complete destruction of the condensate and transformation into an IN. For a state in which the particles are completely localized to the lattice sites, the quasimomentum distribution must be spherically symmetric.

The effect of disorder on the transport properties of the gas is shown in Fig. 3. Data are shown for the COM velocity of the gas along the transverse (v_T) and longitudinal (v_L) directions immediately after an applied impulse for $\Delta=0, 0.75$, and $3 E_R$ and for a range of lattice depths spanning the SF and MI regimes in a clean lattice ($s=6-19$). The technique we employ here is a modification of that used in Ref. 7, in which the dissipation for transport γ is probed by measuring the COM motion of the gas in the parabolic confining potential after applying a spatially uniform impulse. These data are taken in the regime in which the dominant dissipation mechanism in a clean lattice arises from quantum phase slips. We work primarily in the limit of an impulse that is rapid compared with the harmonic motion but not the dissipation rate. In this regime ($\gamma \gg 1/t \gg \omega$), $v = \frac{Ft}{m^*} e^{-\gamma t}$, where F is the force during the impulse of duration t , ω is the oscillator frequency for motion in the parabolic potential, and m^* is the effective mass (which depends on s). Since we fix the impulse Ft for the data in Fig. 3, the emergence of an IN at fixed s is characterized by $\gamma \rightarrow \infty$ and $v = 0$, which is denoted by the dashed line.

In the clean lattice, the velocity approaches the expectation for an IN as the lattice depth is increased into the regime for which atoms in the unit-filling MI state exist in the centre of the lattice. This suppression of the COM velocity for increasing s is caused by an increase in effective mass (characterized by the prediction for $\gamma = 0$,

which is shown by the solid black line) and by an enhancement in the quantum phase slip rate (which scales as $\gamma \propto e^{\sqrt{U/t}}$). The atom gas does not completely transform into an IN when atoms emerge in the MI state because a SF shell always exists at the periphery of the gas²⁶. We find that increasing disorder strength at fixed s generically leads to an increase in γ and corresponding decrease in $|v|$, as indicated by the green arrow and demonstrated in the inset to Fig. 3. The data in the inset for $s = 14$ ($U/t = 44$) are typical for all lattice depths: increasing Δ leads to greater dissipation for motion along either the longitudinal or transverse directions. At $s = 14$, MI and SF phases coexist in the clean lattice. This behaviour therefore conflicts with theories (such as Refs. 9–12) that predict disorder can transform a MI to a SF at $U/t \approx 40$, which would lead to a decrease in γ for increasing Δ .

Although disorder weakly affects transport in the SF regime for $\Delta = 0.75E_R$, increasing the disorder strength to $\Delta = 3E_R$ transforms the SF state to an IN at approximately $s = 12$, corresponding to $U/t = 25$ and $\Delta/U = 10$. Within the systematic uncertainty in determining zero velocity (see Methods), the SF-to-IN transition occurs at the same s for the longitudinal and transverse directions. It is evident from the data in Fig. 3 and the inset that the transition to a disordered IN shifts to lower Δ for higher values of U/t . The plot of condensate fraction N_0/N for $\Delta = 0, 0.75, \text{ and } 3 E_R$ in Fig. 3 shows that the emergence of the disordered insulating state coincides with the obliteration of the condensate and localization of the atoms by disorder. A comparison of the zero temperature prediction from site-decoupled mean-field theory²⁷ for condensate fraction in the clean lattice (solid black line) indicates that our measurements are at low but finite temperature.

In conclusion, the measurements presented in this manuscript suggest the phase diagram shown in Fig. 1c. The primary features we resolve in this work are that disorder can generate a SF-to-IN transition, a disorder-induced IN-to-SF transition is

absent, and that the SF–IN boundary moves to lower Δ for stronger interactions. Our results are most consistent with theoretical approaches that predict the type of phase diagram shown in Fig. 1a, and conflict with those that produce phase diagrams such as Fig. 1b. Direct comparison with theoretical results, however, is complicated by the parabolic potential in experiments and by assumptions about the distributions of BH parameters and temperature in theory. Work in progress by other groups using stochastic mean-field theory, replica theory, and QMC algorithms will enable a more precise assessment of these approaches using our data as a benchmark. We cannot currently distinguish between MI and BG phases. Measurements of the excitation spectrum and compressibility²⁸ of the insulating state we have observed will be necessary before it can be definitively identified as a BG phase.

Methods

We create ⁸⁷Rb BECs using a hybrid magneto-optical trap that is generated using a magnetic quadrupole field and a 1064 nm focused laser beam (see Ref. 6 for details). The average number of atoms is $(12 \pm 4) \times 10^3$, corresponding to 1.4 and 1 particles per site in the centre of the clean lattice for $s = 6$ and 14 according to site-decoupled mean field theory. The ratio U/t is calculated from s using a band structure calculation and the known atomic interaction parameters.

An impulse is applied along the transverse direction via translating the 1064 nm laser beam by $7 \mu\text{m}$ using a trapezoidal ramp that lasts for a total of 3 ms. A uniform magnetic field is applied for 1 ms to create a longitudinal impulse. The magnitude and timing of the magnetic field pulse and the laser beam displacement were adjusted to produce approximately equal impulses along the two directions. We turn off the disordered lattice after the impulse using a $200 \mu\text{s}$ linear ramp of the lattice and speckle light.

The systematic uncertainty in determining zero velocity arises from using a technique to determine this parameter that is unbiased but can result in positive v , which is unphysical given the fixed impulse direction. We set zero velocity by measuring the COM position x_0 of the NC without an applied impulse. We correct for a systematic shift in x_0 that depends on Δ arising from a slight misalignment of the speckle field with respect to the centre of the lattice. We also observe a weak systematic dependence of x_0 on s . The ± 0.15 mm/s systematic uncertainty shown in Fig. 3 is equivalent to the spread in x_0 for all s and Δ used in this work. The measured velocity of the condensate and NC components after the impulse is determined by the displacement from x_0 following 20 ms TOF. The COM velocity is defined as $v = (v_0 N_0 / N_{NC} + v_{NC}) / (1 + N_0 / N_{NC})$, where v_0 and v_{NC} are the condensate and NC velocities, and N_0 and N_{NC} are the numbers of condensate and NC atoms.

This work was supported by the DARPA OLE program (ARO award W911NF-08-1-0021), the Sloan Foundation, and the National Science Foundation (award 0448354). D. McKay acknowledges support from NSERC.

Correspondence and requests for materials should be addressed to B. DeMarco (bdemarco@illinois.edu)

- ¹ Chan, M. H. W., Blum, K. I., Murphy, S. Q., Wong, G. K. S. & Reppy, J. D. Disorder and the Superfluid Transition in Liquid ^4He . *Phys. Rev. Lett.* **61**, 1950-1953 (1988).
- ² Goldman, A. M. Superconductor-insulator transitions in the two-dimensional limit. *Physica E* **18**, 1-6 (2003).
- ³ Phillips, J. C., Saxena, A. & Bishop, A. R. Pseudogaps, dopants, and strong disorder in cuprate high-temperature superconductors. *Rep. Prog. Phys.* **66**, 2111-2182 (2003).
- ⁴ Lewenstein, M. *et al.* Ultracold atomic gases in optical lattices: mimicking condensed matter physics and beyond. *Adv. Phys.* **56**, 243-379 (2007).
- ⁵ White, M. *et al.* Strongly interacting bosons in a disordered optical lattice. *Phys. Rev. Lett.* **102**, 055301 (2009).
- ⁶ McKay, D., White, M. & DeMarco, B. Lattice Thermodynamics for Ultra-Cold Atoms. *Phys. Rev. A* **79**, 063605 (2009).
- ⁷ McKay, D., White, M., Pasienski, M. & DeMarco, B. Phase-slip-induced dissipation in an atomic Bose-Hubbard system. *Nature* **453**, 76-79 (2008).

- 8 Trivedi, N. Quantum Phase Transition in Disordered Systems: What are the
Issues? in *Proceedings of the 20th International Workshop on Condensed
Matter Theories* Vol. **12**, 141-157 (Plenum Press, 1997).
- 9 Bissbort, U. & Hofstetter, W. Stochastic mean-field theory for the disordered
Bose-Hubbard model. *arxiv:0804.0007* (2008).
- 10 Wu, J. & Phillips, P. Minimal model for disorder-induced missing moment of
inertia in solid ^4He . *Phys. Rev. B* **78**, 014515 (2008).
- 11 Pollet, L., Prokof'ev, N. V., Svistunov, B. V. & Troyer, M. Absence of a Direct
Superfluid to Mott Insulator Transition in Disordered Bose Systems.
arxiv:0903.3867 (2009).
- 12 Kruger, F., Wu, J. & Phillips, P. Anomalous suppression of the Bose glass at
commensurate fillings in the disordered Bose-Hubbard mode. *arxiv:0904.4480*
(2009).
- 13 Fisher, M. P. A., Weichman, P. B., Grinstein, G. & Fisher, D. S. Boson
Localization and the Superfluid-Insulator Transition. *Phys. Rev. B* **40**, 546-570
(1989).
- 14 Rapsch, S., Schollwock, U. & Zwerger, W. Density matrix renormalization
group for disordered bosons in one dimension. *Europhys. Lett.* **46**, 559-564
(1999).
- 15 Krauth, W., Trivedi, N. & Ceperley, D. Superfluid-insulator transition in
disordered boson systems. *Phys. Rev. Lett.* **67**, 2307-2310 (1991).
- 16 Giamarchi, T. & Schulz, H. J. Localization and Interaction in One-Dimensional
Quantum Fluids. *Europhys. Lett.* **3**, 1287-1293 (1987).
- 17 Damski, B., Zakrzewski, J., Santos, L., Zoller, P. & Lewenstein, M. Atomic
Bose and Anderson glasses in optical lattices. *Phys. Rev. Lett.* **91**, 080403
(2003).
- 18 Lye, J. E. *et al.* Bose-Einstein condensate in a random potential. *Phys. Rev. Lett.*
95, 070401 (2005).
- 19 Chen, Y. P. *et al.* Phase coherence and superfluid-insulator transition in a
disordered Bose-Einstein condensate. *Phys. Rev. A* **77**, 033632 (2008).
- 20 Clement, D. *et al.* Suppression of transport of an interacting elongated Bose-
Einstein condensate in a random potential. *Phys. Rev. Lett.* **95**, 170409 (2005).
- 21 Schulte, T. *et al.* Routes towards Anderson-like localization of Bose-Einstein
condensates in disordered optical lattices. *Phys. Rev. Lett.* **95**, 170411 (2005).
- 22 Billy, J. *et al.* Direct observation of Anderson localization of matter waves in a
controlled disorder. *Nature* **453**, 891-894 (2008).
- 23 Roati, G. *et al.* Anderson localization of a non-interacting Bose-Einstein
condensate. *Nature* **453**, 895-898 (2008).
- 24 Gerbier, F. *et al.* Phase Coherence of an Atomic Mott Insulator. *Phys. Rev. Lett.*
95, 050404 (2005).
- 25 Scalettar, R. T., Batrouni, G. G. & Zimanyi, G. T. Localization in interacting,
disordered, Bose systems. *Phys. Rev. Lett.* **66**, 3144-3147 (1991).
- 26 DeMarco, B., Lannert, C., Vishveshwara, S. & Wei, T.-C. Structure and stability
of Mott-insulator shells of bosons trapped in an optical lattice. *Phys. Rev. A* **71**,
063601 (2005).
- 27 Sheshadri, K., Krishnamurthy, H. R., Pandit, R. & Ramakrishnan, T. V.
Superfluid and insulating phases in an interacting-boson model: Mean-field
theory and the RPA. *Europhys. Lett.* **22**, 257-263 (1993).

- ²⁸ Delande, D. & Zakrzewski, J. Compression as a Tool to Detect Bose Glass in a Cold Atomic Gas. *Phys. Rev. Lett.* **102**, 085301 (2009).
- ²⁹ Pollet, L., Svistunov, B. & Prokof'ev, N. private communication.

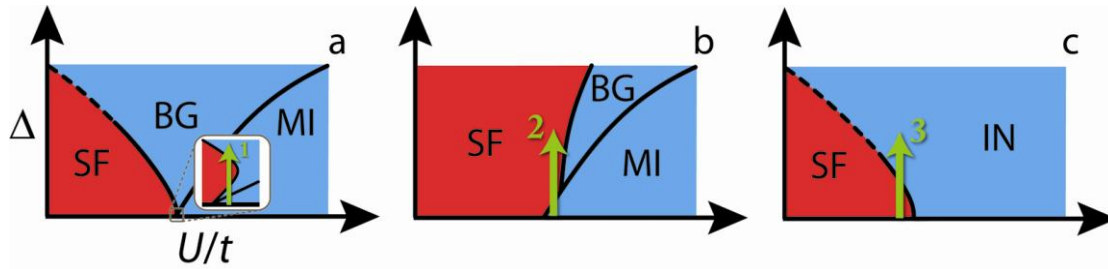


Figure 1. Phase diagrams for the DBH model. a,b, Predicted phase diagrams for the DBH model at unit site filling broadly fall into two categories, shown schematically. For both cases, SF (red) and insulating (blue) MI and BG phases emerge at zero temperature as the disorder strength Δ and ratio of Hubbard interaction energy U to tunnelling energy t are varied. For type **a**, the SF and MI phases do not share a boundary for any non-zero Δ , and the SF–BG boundary at low U/t is not well known in three dimensions (indicated by the dashed line). The inset to **a** shows that a disorder driven BG–SF transition is possible in a narrow range of U/t and Δ (1), although this feature is likely absent at non-zero temperature²⁹. In phase diagrams of class **b**, the SF and MI phases share a boundary at finite Δ , and disorder can induce a MI–SF transition (2), typically at $U/t \approx 40$ in three-dimensions. Another primary difference between **a** and **b** is the behaviour of the SF–IN boundary: **a**, the boundary moves to higher Δ for lower U/t ; **b**, the boundary shifts to higher Δ for increasing U/t . **c**, The phase diagram suggested by our data, in which only a disorder-induced SF–IN transition is possible (3) and the SF–IN boundary behaves as in **a**; we cannot distinguish between BG and MI phases at present.

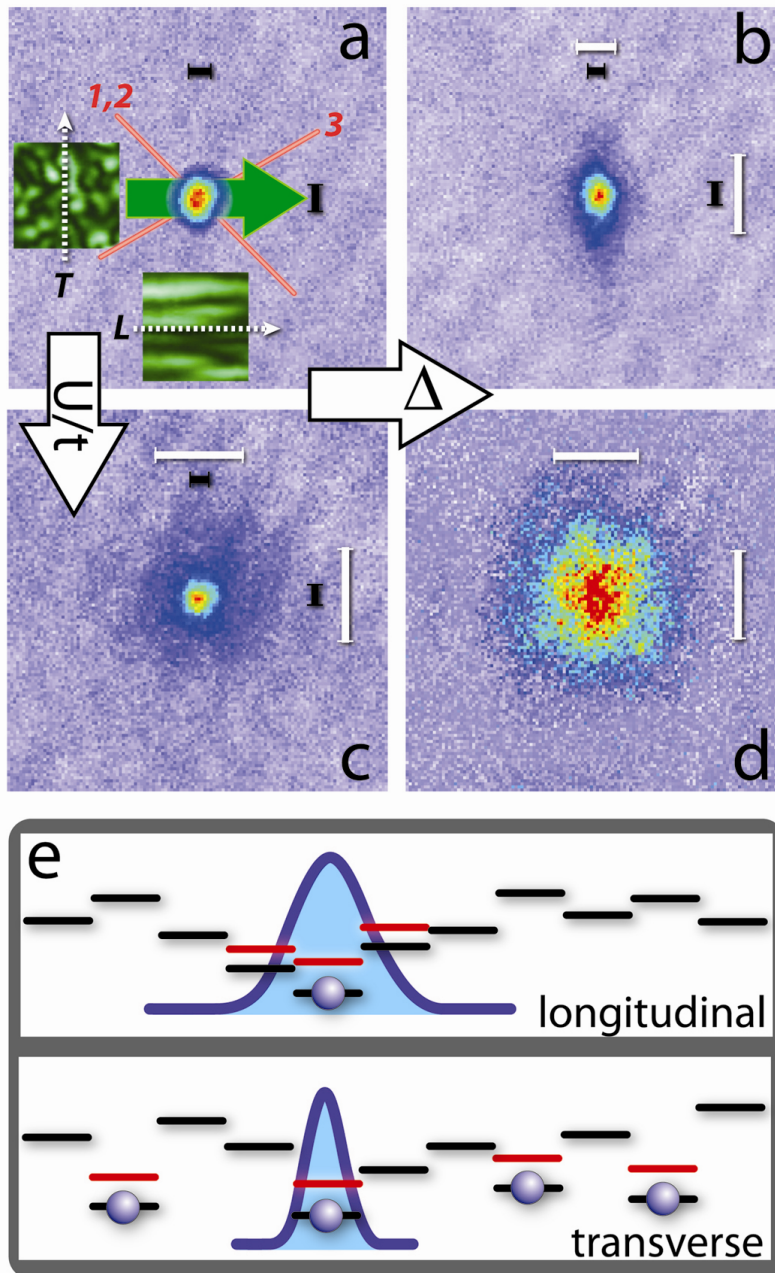


Figure 2. Effect of disorder on quasimomentum distribution and evidence for disorder-induced localization. **a–d**, Images taken after bandmapping from the disordered lattice and TOF are shown in false colour for **a**, $s=6$, $\Delta=0$; **b**, $s=6$, $\Delta=3E_R$; **c**, $s=12$, $\Delta=0$; and **d**, $s=12$, $\Delta=3E_R$. The TOF is 25 ms for $s=6$ and 15 ms for $s=12$; the field-of-view for each image is 0.6 mm. The images are fit to two-component Gaussian distributions to determine condensate fraction and the sizes and locations of the condensate and NC.

The black and white bars correspond to twice the fitted r.m.s. radius for the condensate and NC components. The reduction in condensate fraction from **a** to **c** as the interaction strength is increased is caused by quantum depletion. The broad quasimomentum distribution observed in **d** when strong disorder is applied in the quantum depleted SF regime implies that disorder is localizing the atoms and giving rise to an IN. **e**, A simple model that may be used to understand the effect of disorder on the quasimomentum distribution. Atoms (blue spheres) localize to regions (blue curves) to screen the disordered potential and create a more uniform effective potential.

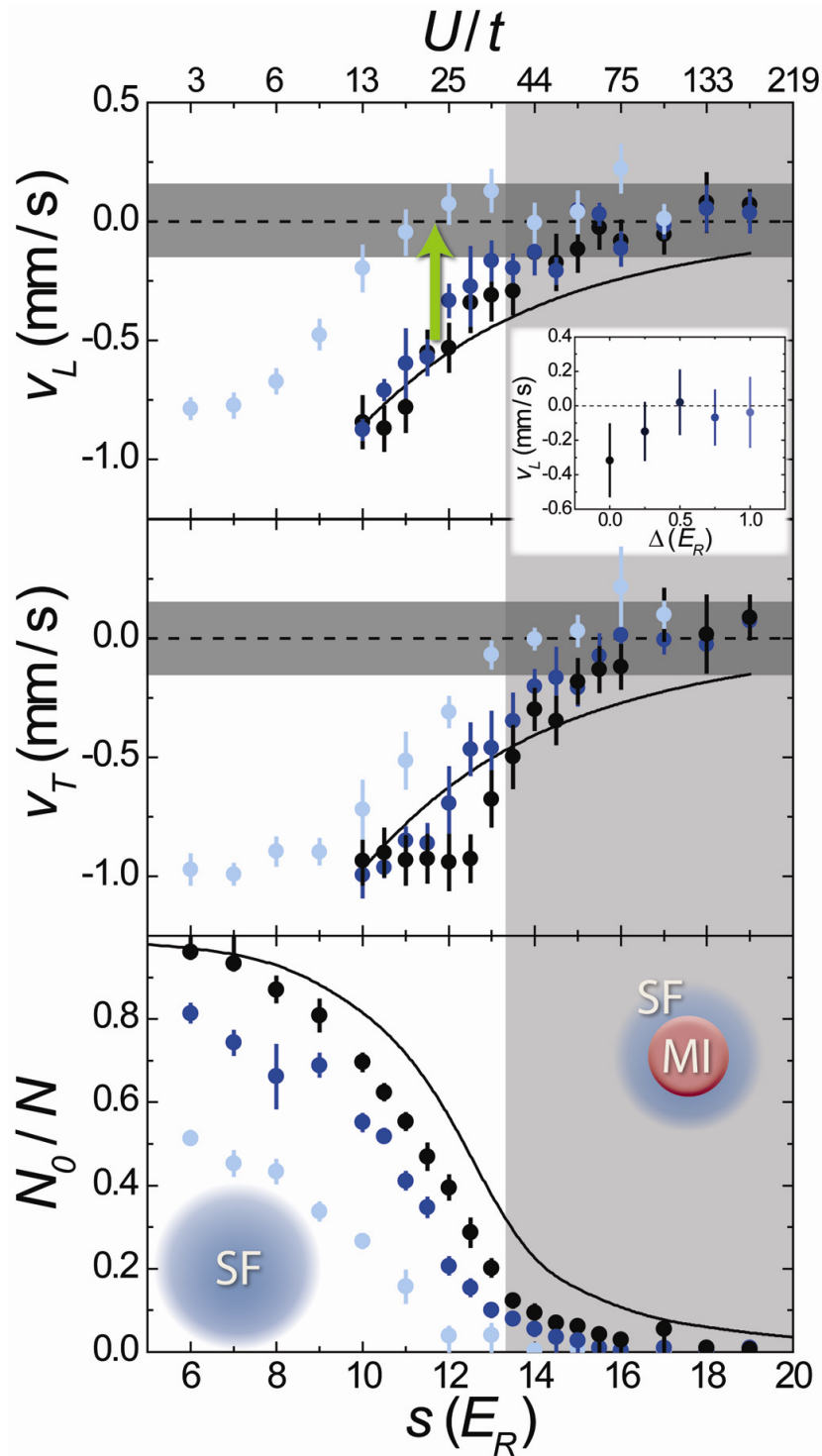


Figure 3. Effect of disorder on transport and condensate fraction. The overall COM velocity v of the gas after an impulse is applied is plotted as the

lattice depth s is varied for three disorder strengths: $\Delta = 0$ (black), 0.75 (dark blue), and $3.0 E_R$ (light blue); data are shown for the longitudinal (top) and transverse (middle) directions. The inset shows how disorder affects v_L for $s = 14$; the colour scale for the points follows the main figure for reference. Within the region marked in light grey, a spherical core of unit filling MI exists in the centre of the lattice (according to 3D mean field theory). The dark grey band indicates the systematic uncertainty in determining zero velocity (see Methods). The error bars represent the statistical uncertainty in the (typically) seven measurements averaged for each point. The error bars for v also include the statistical uncertainty in determining zero velocity, and the error bars for N_0 / N include a systematic error that reflects our inability to measure condensate fraction above 95% and below 5%.